Macromolecules
ARTICLE

Macromolecules **2009**, *42*, 5043–5052 **5043**
DOI: 10.1021/ma900715c

Reversible Addition−Fragmentation Chain Transfer (RAFT) Polymerization in an Inverse Microemulsion System: Homopolymerization, Chain Extension, and Block Copolymerization†

Atsushi Sogabe‡ and Charles L. McCormick*,‡,§

‡*Department of Polymer Science and* §*Department of Chemistry and Biochemistry, The University of Southern Mississippi, Hattiesburg, Mississippi 39406*

Received April 2, 2009; Revised Manuscript Received June 9, 2009

ABSTRACT: We report the first successful reversible addition−fragmentation chain transfer inverse microemulsion polymerization (RAFT-IMEP). The inverse microemulsion (IME) system conditions were optimized by generating pseudo-three-component phase diagrams. The IME consisted of the hydrophilic monomer *N,N*-dimethylacrylamide (DMA), water, hexanes, nonionic surfactants, and a cosurfactant. The polymerization kinetics and the living character of RAFT-IMEP, conducted with varying amounts of dispersed aqueous phase, were similar to that observed for aqueous RAFT polymerization of DMA. The colloidal stability during polymerization was also investigated via dynamic light scattering. Decreasing the weight fraction of the dispersed aqueous phase leads to an increase in colloidal stability and a decrease in microemulsion size. An increase in the dispersity of molecular weight is also observed with a decrease in the weight fraction of dispersed aqueous phase. This observation is attributed to uncontrolled polymer that forms during the early stages of RAFT-IMEP. Chain extension or block copolymer formation is accomplished by simple addition of DMA or DEA to the polyDMA macroCTA, demonstrating the potential utility for preparing doubly hydrophilic block copolymers under appropriate RAFT/IMEP conditions.

Introduction

The recent progress in controlled/"living" radical polymerization techniques has provided impetus for synthesizing well-defined polymers with advanced architectures. Such techniques include nitroxide-mediated polymerization (NMP),[1] atom transfer radical polymerization (ATRP),[2] and reversible addition−fragmentation chain transfer (RAFT) polymerization.[3−6] Among these techniques, RAFT polymerization is arguably the most versatile since it is compatible with a wide variety of functional monomers under mild reaction conditions.[7,8] The robust nature of the RAFT process has allowed significant progress in the area of aqueous RAFT polymerization.[5,6] Our group, having a long-standing interest in water-soluble functional polymers, has recently focused on controlled polymerization of anionic,[9] cationic,[10,11] zwitterionic,[12] and neutral[13,14] monomers utilizing aqueous RAFT polymerization.

Emulsion polymerization is often used in large-scale production of polymers due to the facile control of reaction kinetics, ease of product isolation, and subsequent application. Emulsion systems are generally classified as one of the following types: macroemulsion (the most common), miniemulsion, and microemulsion. These systems differ fundamentally in the dimensions of the dispersed phase. While the diameters of the dispersed phase in macroemulsions are typically greater than 1 μm,[15] miniemulsions (50−500 nm)[16,17] and microemulsions (10−100 nm)[15] are on the nanometer scale. Although mini- and microemulsions overlap in the size of the dispersed phase, these two systems are significantly different in terms of stability. Miniemulsions are generated by vigorous stirring, followed by ultrasonication and are thermodynamically unstable microphase systems that will eventually phase separate. Microemulsions, on the other hand, are generated spontaneously without the necessity of vigorous agitation and are thermodynamically stable. However, it is often difficult to find conditions for generating stable microemulsions, since the type and relative concentrations of surfactants, cosurfactant, continuous phase, and other components must be carefully determined.

Since the discovery of RAFT, many researchers have attempted polymerization in emulsion systems.[7,18−29] The first reported attempt of RAFT macroemulsion polymerization was by Le et al., obtaining polystyrene with molecular weight of 53 200 and a PDI of 1.37.[18] Later work utilizing RAFT macroemulsion polymerization revealed problems of rate retardation, phase separation, and loss of livingness.[20,21,25,28,30] These difficulties have been attributed to the diffusion of the chain transfer agent (CTA) or oligomeric CTA into and out of the emulsion particles.[25,31] Furthermore, the ratio of monomer to CTA concentration in the macroemulsion is not constant during polymerization due to differences in their respective diffusion coefficients.[32] To limit the diffusion of the CTA, seeded emulsion,[33,34] starved fed,[35] oligomeric CTA,[26,36] and ab initio emulsion polymerization techniques[27,37,38] have been implemented. However, these techniques can be laborious since each usually involves multistep reactions. Because of the difficulties associated with RAFT macroemulsion polymerization, several groups have turned to miniemulsion systems since each monomer droplet can, in principle, serve as a locus of polymerization without the diffusion of monomer and CTA.[19,22,39,40] In some instances, phase separation of oligomeric CTA occurs, which has been termed "superswelling".[20,39] The reported problems associated with RAFT macro- and miniemulsion polymerizations have led to investigations of the alternative microemulsion systems which should have thermodynamic stability.[41]

† Paper no. 140 in a series on Water-Soluble Polymers.

*To whom correspondence should be addressed. E-mail: Charles.McCormick@usm.edu.

Published on Web 07/02/2009

Scheme 1

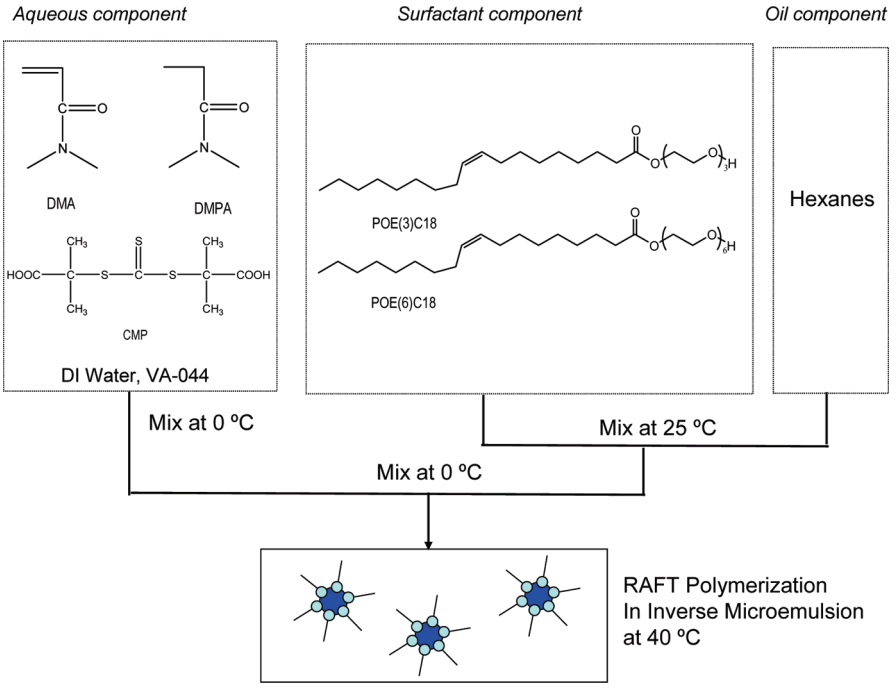

The RAFT polymerizations discussed above are all based on oil-in-water emulsions and are not applicable for synthesizing hydrophilic polymers. Compared to the oil-in-water emulsion systems, a minimal number of inverse emulsion systems have been reported.[42−50] Our literature survey reveals only one report regarding RAFT inverse miniemulsion polymerization[51] and none regarding RAFT inverse microemulsion polymerization (RAFT-IMEP). For the former, experimental molecular weights matched with the theoretical values at conversions less than 40% using a hydrophilic initiator. At higher conversion, experimental molecular weights were greater than the predicted values, and this is attributed to the hydrolysis of CTA. Moreover, the colloidal stability of the system was not discussed.

In this report, we describe, to our knowledge, the first successful RAFT-IMEP. The inverse microemulsion system was obtained by carefully constructing pseudo-three-component phase diagrams. This system includes DMA as the hydrophilic monomer, nonionic surfactants, and a cosurfactant. The kinetic behavior and the living character of RAFT-IMEP, with systematic variation of the dispersed aqueous phase, were compared to those of RAFT aqueous solution polymerization. The colloidal stability of the microemulsion during polymerization was also investigated via dynamic light scattering. Chain extension with DMA and block copolymerization with DEA were successfully performed from the polyDMA macroCTA, indicating the utility of this method in preparing block copolymers including doubly hydrophilic and/or amphiphilic systems.

Experimental Section

Materials. *N,N*-Dimethylacrylamide (DMA), *N,N*-diethylacrylamide (DEA), and *N,N*-dimethylpropionamide (DMPA) (Aldrich, Milwaukee, WI) were distilled under reduced pressure. Polyoxyethylene(3) oleyl ether (POE(3)C18), polyoxyethylene (6) oleyl ether (POE(6)C18) (Nihon Emulsion, Tokyo, Japan), and hexanes (Aldrich, Milwaukee, WI) were used as received. 2,2′-Azobis[2-(2-imidozolin-2-yl)propane] dihydrochloride (VA-044) was used as the initiator (gifts from Wako Chemicals USA, Inc.) The difunctional CTA 2-(1-carboxy-1-methylethylsulfanylthiocarbonylsulfanyl)-2-methylpropionic acid (CMP) was used without further purification (gift from Noveon, Inc.).

Preparation of Pseudo-Three-Component Phase Diagrams. The following three components were used to generate phase diagrams. The oil component consisted of hexanes, the surfactant component consisted of 33.3 wt % of POE(3)C18 and 66.7 wt % of POE(6)C18, and the aqueous component consisted of (a) DI water, (b) 20 wt % DMA, (c) 20 wt % DMPA, or (d) 20 wt % DMA and 20 wt % DMPA and a small amount of CMP. These three components were mixed at various ratios and left at 40 °C for 2 h. The phase diagrams were generated from visual inspection and conductivity measurements of the resulting mixtures.

RAFT Polymerization of DMA in Inverse Microemulsion. General Procedure (Scheme 1). *Aqueous Component*. CMP (14.2 mg, 5.05 mmol) was dissolved in DMA (2.00 g, 20.2 mmol) and DMPA (2.00 g, 19.8 mmol) in a 20 mL vial. DI water (5.00 g) was then added to the solution and cooled to 0 °C. A stock solution cooled to 0 °C containing VA-044 (3.26 mg, 1.01 mmol) and DI water (1.00 g) was added to the vial. The solution was stirred and purged with N_2 for 1 h at 0 °C.

Mixture of Oil Component and Surfactant Component. Hexanes (8.75 g), POE(3)C18 (0.700 g), and POE(6)C18 (1.40 g) were added to a 20 mL round bottle flask. The solution was stirred and purged with N_2 for 1 h at 25 °C and then cooled to 0 °C.

Preparation of Inverse Microemulsion (IME) and RAFT Polymerization. The aqueous component (1−4 g) was added to the oil and surfactant mixture at 0 °C under N_2. The solution was purged with N_2 for another 1 h and then was immersed oil bath at 40 °C. The inverse microemulsion was generated within 10 min after heating. The reaction was terminated after 20 h by cooling to 0 °C in an ice bath followed by exposure to air. The polymerization kinetics were monitored by taking aliquots at predetermined time intervals utilizing degassed syringes. Monomer concentration was determined by UV absorbance at 260 nm. GPC was used to determine the molecular weight at different time intervals while UV absorbance at 310 nm was utilized to detect the CTA moiety.

Chain Extension in a One-Pot System. The polyDMA with target DP = 100 was synthesized (10 h, ∼100% conversion) by RAFT-IMEP with an 8.5 wt % aqueous component as described above. An additional monomer solution containing DMA (0.20 g, 2.02 mmol) and DMPA (0.20 g, 1.98 mmol) was prepared and purged with N_2 at 0 °C for 1 h. This second

batch of monomer was added into the IME mixture under N_2. The chain extension was conducted for another 10 h at 40 °C to yield a final target DP of 200.

Block Copolymerization in a One-Pot System. The polyDMA with target DP = 100 was synthesized (10 h, ~100% conversion) by RAFT-IMEP with an 8.5 wt % aqueous component as described above. DEA (0.272 g, 2.14 mmol) as the second monomer was purged with N_2 at 0 °C for 1 h. This second batch of monomer was added into the IME mixture under N_2. The block copolymerization was conducted for another 6 h at 40 °C to yield a final target of poly(DMA_{50}-DEA_{106}-DMA_{50}).

Gel Permeation Chromatography. After the polymerization, hexanes were removed from the mixture by purging with N_2 gas. Ethanol was added to dissolve the mixture, and then surfactants were separated by using centrifugal filtration (MWCO 3000, Ultracel YM-3 or MWCO 10 000 Ultracel YM-10). Following filtration, the samples were analyzed by aqueous size exclusion chromatography (ASEC) using an eluent of 20%/80% acetonitrile/0.05 M Na_2SO_4 at a flow rate of 0.3 mL/min at 25 °C. This instrument was equipped with TOSOH Biosciences TSK-GEL columns [Supre AW3000 G3000 PWXL (< 50 000 g mol^{-1}, 200 A) and G4000 PWXL (2000−300 000 g mol^{-1}, 500A)], a Polymer Laboratories LC 1200UV/vis, Wyatt Optilab DSP interferometric refractometer, and Wyatt DAWN EOS multiangle laser light scattering detectors (690 nm). The dn/dc of PDMA (0.1645 mL/g) in the above eluent was determined at 25 °C. M_n, M_w, and polydispersity indices (PDIs) for polymers were determined.

After hexanes were removed from the polymerization mixture by purging with N_2 gas, the molecular weights and PDI of the copolymers were determined by size exclusion chromatography using 0.05 M ammonium acetate in DMF as eluent at a flow rate of 1.0 mL/min at 35 °C. This instrument was equipped with Viscotek I-Series Mixed Bed low-MW and mid-MW columns, Viscotek-TDA (302 nm RI, viscosity, 7 mW 90° and 7° true low angle light scattering detectors (670 nm). The dn/dc of PDMA (0.0842 mL/g) in the above eluent was determined at 35 °C using a Viscotek refractometer and Omnisec software.

Dynamic Light Scattering. Dynamic light scattering was conducted using a Malvern Instruments Zetasizer Nano series instrument equipped with a 22 mW He−Ne laser operating at $\lambda = 632.8$ nm, an Avalanche photodiode detector with high quantum efficiency, and an ALV/LSE-5003 multiple tau digital correlator electronics system. The diameters of the IMEs were directly measured without filtering the mixtures.

Calculation of the Number of CTAs in Each Particle. The number of CTAs (N) in each particle was calculated using eq 1 in which

$$N = \frac{4\pi r^3}{3}\frac{d w_c N_A}{M} \quad (1)$$

r is the radius of the IME, d is the density of aqueous phase (1.014 g/cm^3), w_c is the weight fraction of CTA in aqueous phase (0.001 422 g/g), M is the molecular weight of CTA (282.4 g/mol), and N_A is Avogadro's number.

Results and Discussion

A review of the literature reveals a large number of papers describing conventional water-in-oil (W/O) microemulsion polymerization; however, relatively few studies have been carried out utilizing inverse microemulsion polymerization (IMEP)[42−50] and none involving RAFT-IMEP. One of the reasons is difficulty in formulation and loading of micelles with sufficient stability in the organic external phase. Since the size of the ionic hydrophilic groups tend to be compact, ionic surfactants are mainly used.[42−49] However, the use of ionic surfactants has been limited to combinations with nonionic monomers. Charged monomers associate with oppositely charged ionic surfactants, causing precipitation. Kaneda et al. studied inverse microemulsion polymerization (IMEP) of poly(AMPS-*co*-DMA) with nonionic surfactants.[52,53] Their system allowed the formation of stable IMEs containing more than 40% aqueous phase, and in addition, IME size could be varied by changing the amount of aqueous phase. We employed a similar surfactant system in our study and have shown that by varying the ratio of the components phase diagrams can be dramatically altered. In accordance, pseudo-three-component phase diagrams have been generated to establish conditions for optimal formulation of IMEs suitable for RAFT polymerization.

Preparation of Pseudo-Three-Component Phase Diagrams. Generally PEO-based nonionic surfactants are thermoresponsive at the phase inversion temperature (PIT).[54,55] Below the PIT, O/W emulsions are formed. Raising the temperature of the mixture to above the PIT generates W/O emulsions, also known as inverse emulsions. At temperatures near the PIT, surface tension is minimized, and thus either O/W or W/O microemulsions can be generated without mechanical stirring. Thus, variation in temperature is a practical method for obtaining microemulsions and IMEs. The PIT depends not only on the PEO-based surfactant but also on the type of monomer, cosurfactant, organic solvent, and salt concentration. In this study the PIT was ~40 °C, and all experiments were conducted at this temperature.

To obtain IMEs, pseudo-three-component phase diagrams consisting of aqueous, oil, and surfactant components were generated as illustrated for example in Figure 1. In these phase diagrams, the aqueous component consists of (a) DI water, (b) 20 wt % DMA, (c) 20 wt % DMPA, and (d) 20 wt % DMA and 20 wt % DMPA. The borderline between O/W and W/O emulsions was determined by conductivity measurements. Focusing on the inverse (W/O) region in Figure 1a, four phases are observed. Without the aqueous component, the surfactant mixture is not completely dissolved in the oil phase, resulting in two phases consisting of oil and insoluble surfactant (D + O). When a small weight fraction of aqueous component is added, an IME (indicated as inverse micelle, O_m) is obtained in a narrow region. The IME can only contain 8.5 wt % aqueous component. Increasing the aqueous component above 15.6 wt % results in a mixture of IME and excess aqueous phase (O_m + W). When the concentration of surfactant is too high, a mixture of oil gel and aqueous component (O_{gel} + W) is obtained. When the aqueous phase consists of 20 wt % DMA, the IME region expands (Figure 1b). Generally, alcohols, amides, and other polar organic chemicals are used as a cosurfactant to help generate a microemulsion or an IME. It has been suggested that DMA works as a cosurfactant in a similar manner to acrylamide.[44,56] However, when the DMA concentration decreases during the polymerization, it is possible that the integrity of the IME can be lost. To keep the IME intact during polymerization, a cosurfactant that is not consumed during polymerization must be utilized. Several alcohols, amides, DMSO, *N,N*-dimethylformamide (DMF), and DMA analogues were tested as cosurfactants and were compared to DMA. It was found that *N,N*-dimethylpropionamide (DMPA) expands the IME region, a behavior similar to DMA (Figure 1c). Furthermore, when both DMA and DMPA were used as cosurfactants, an even wider IME region is generated (Figure 1d).

The weight fractions of aqueous component used for RAFT-IMEP were 39.3, 21.7, 15.6, and 8.5 wt %. For the first system, the IME is outside the O_m region when all DMA is consumed (Figure 1c,d), leading to mixed (O_m + W). The other three systems, however, have stable O_m regions after polymerization.

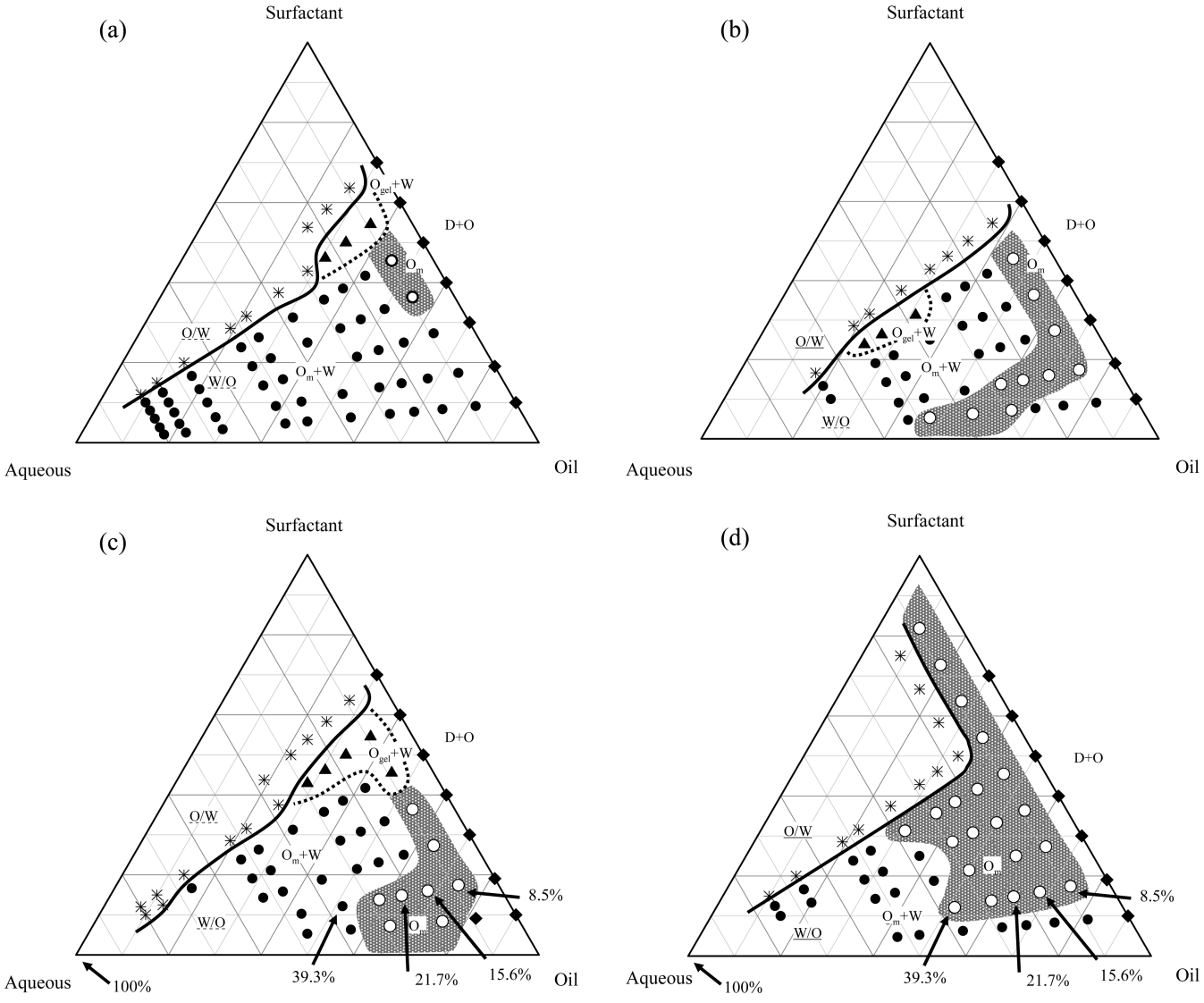

Figure 1. Pseudo-three-component phase diagrams. Oil phase was hexanes, surfactant phase consisted of 33.3 wt % of POE(3)C18 and 66.7 wt % of POE(6)C18, and aqueous phase was (a) DI water, (b) 20 wt % DMA aqueous solution, (c) 20 wt % DMPA aqueous solution, or (d) 20 wt % DMA and 20 wt % DMPA aqueous solution. The solid line designates the border between O/W and W/O. O_m (○): inverse micelle or inverse microemulsion (transparent); O_m + W (●): inverse microemulsion + excess aqueous phase (W/O emulsion, milky); O_{gel} + W (▲): oil gel + excess aqueous phase (translucent); D + O (♦): surfactant and oil, O/W type (∗).

RAFT Inverse Microemulsion Polymerization (RAFT-IMEP). RAFT-IMEPs were conducted using the conditions discussed above and utilizing component weight fractions shown in Table 1. Entries 2−5 have the same target molecular weight; the molar ratios of monomer:CTA:initiator were fixed at 400:1:0.2. In these experiments, the weight fractions of aqueous phase were varied. The sizes of the IMEs before polymerization were found to be 10−40 nm by dynamic light scattering (DLS), and these emulsions were transparent or bluish. The experimental data after 20 h of polymerization are shown in Table 2, and the GPC chromatograms are shown in Figure 2. Conversions reach nearly 100% under all conditions, and experimental molecular weights are close to the theoretical values. The polydispersities (PDIs) are below 1.2, except for entry 5. It appears that the PDI increases with decreasing aqueous phase. This phenomenon will be discussed in more detail later. When the aqueous content is 39.3 wt % (entry 2), precipitation and phase separation are observed with a broad particle size distribution. Therefore, the particle diameter cannot be determined in this case. During the polymerization, consumption of DMA in the phase diagram shown in Figure 1d becomes like that in Figure 1c. In Figure 1c, entry 2 is not in the IME region. The colloidal instability of the IMEP with 39.3 wt % aqueous phase can be attributed to the consumption of DMA. Except for entry 2, DLS measurements reveal unimodal particle size distributions before and after polymerization as shown in Figure 3. However, an increase in the diameters of the IME is observed after the completion of polymerization. Ideally, every IME should be converted to an IME polymer particle. However, only a fraction of the inverse micelles nucleate, and the remaining inverse micelles provide monomer to the growing IME polymer particles.[44,57] Generally, the number of particles decreases to 1/1000th of the original number of inverse micelles at the start polymerization. Consequently, polymer particle size becomes larger after polymerization.[41,58] It is thought that the transportation of monomer causes the observed increase in the emulsion size during polymerization. Polymer emulsions of entries 3−5 have unimodal size distribution after polymerization. No aggregation and coalescence of entry 5 is observed after 2 months at ambient temperature. Polymer

Table 1. Recipe for RAFT Inverse Microemulsion Polymerization of DMA

	aqueous component					oil component	surfactant component		
entry	DMA (g)	DMPA (g)	CMP (mg)	VA-044 (mg)	DIW (mg)	hexanes (g)	POE(3)C18 (g)	POE(6)C18 (g)	frac of aq (wt %)
1	2.00	2.00	14.24	3.26	6.00				100.0
2	1.40	1.40	9.97	2.28	4.20	8.75	0.70	1.40	39.3
3	0.60	0.60	4.27	0.98	1.80	8.75	0.70	1.40	21.7
4	0.40	0.40	2.85	0.65	1.20	8.75	0.70	1.40	15.6
5	0.20	0.20	1.42	0.33	0.60	8.75	0.70	1.40	8.5
6	0.20	0.20	2.85	0.65	0.60	8.75	0.70	1.40	8.5
7	0.20	0.20	5.70	1.30	0.60	8.75	0.70	1.40	8.5
8	0.40	0.40	5.70	1.30	0.60	8.75	0.70	1.40	12.1

Table 2. Resuls for RAFT Inverse Microemulsion Polymerization of DMA

entry		frac of aq (wt %)	conv (%)	M_n(theory) (kg mol^{-1})	M_n(expt) (kg mol^{-1})	M_w/M_n	D (t = 0) (nm)	D (t = 20 h) (nm)
1	solution	100.0	94.9	37.9	35.7	1.14		
2	IMEP	39.3	99.8	39.9	38.3	1.15	34.1	polydisperse
3	IMEP	21.7	99.9	39.9	34.6	1.19	19.5	523.2
4	IMEP	15.6	99.5	39.7	43.1	1.20	18.3	239.3
5	IMEP	8.5	96.5	38.6	40.0	1.68	11.9	82.7
6	IMEP	8.5	92.2	18.6	17.3	1.36	11.3	114.3
7	IMEP	8.5	96.1	9.8	11.8	1.29	11.7	122.4

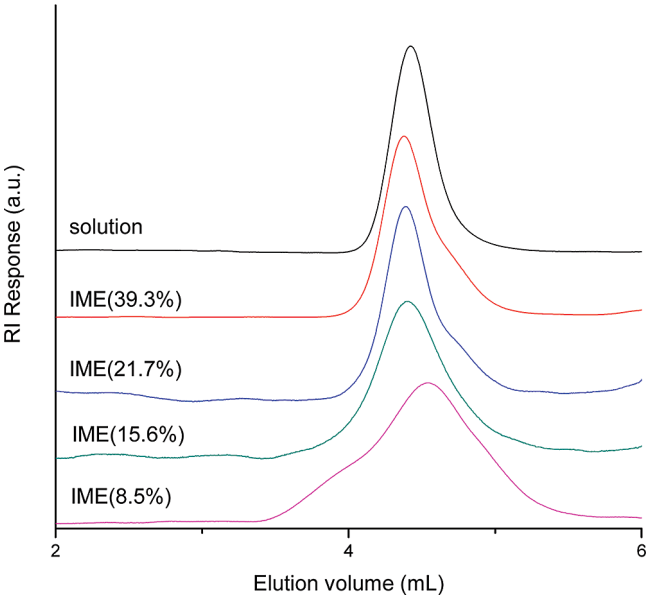

Figure 2. Chromatograms of polyDMA synthesized by RAFT solution (94.9% conversion) and RAFT-IMEP using different weight fractions of aqueous phase (39.3 wt % (99.8% conversion), 21.7 wt % (99.9% conversion), 15.6 wt % (99.5% conversion), 8.5 wt % (96.5% conversion)).

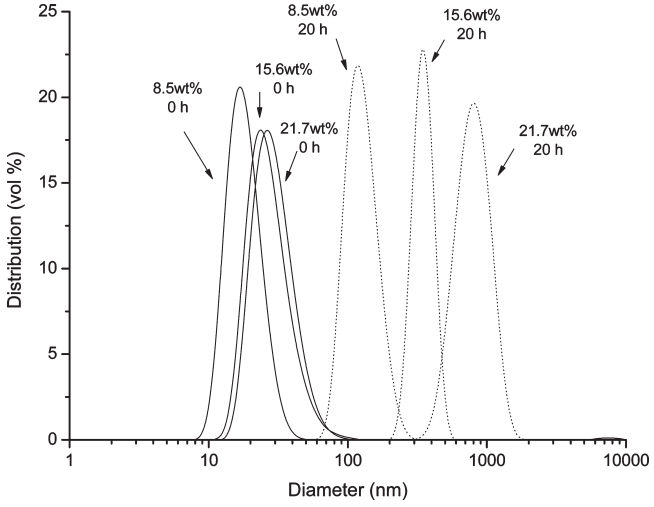

Figure 3. Hydrodynamic size distribution of inverse microemulsions: (a) IME 8.5 wt % at 0 h, (b) IME 15.6 wt % at 0 h, (c) IME 21.7 wt % at 0 h, (d) IME 8.5 wt % at 20 h, (e) IME 15.6 wt % at 20 h, (f) IME 21.7 wt % at 20 h.

emulsions of entries 3 and 4 precipitated after a few weeks; however, these are easily dispersed with gentle agitation. The favorable conditions discussed above were subsequently used in the study the polymerization kinetics of DMA by RAFT-IMEP.

Kinetic Studies of RAFT-IMEP. Considering nonliving radical polymerization in emulsion systems, the rate of polymerization is thought to be increased by zero-one kinetics based on Smith−Ewart theory.[59] However, for controlled/living radical polymerization, other effects have been suggested.[60−67] When controlled/living radical polymerization is conducted in a confined space such as a miniemulsion or microemulsion in which reaction species do not diffuse, two types of compartmentalization effects have been suggested: a segregation effect and a confined effect.[58,61−67] The confined effect refers to two species located in the same particle reacting at higher rate in a small particle as compared to a larger particle.[60−64] Theoretically, the confined effect is only operative on deactivation of ATRP and NMP which involve the activation−deactivation process[58,60−63] and is not operative on RAFT.[58,60,64] Hence, the rate of polymerization decreases with decreasing size of the emulsion. On the contrary, the segregation effect refers to two species located in separate particles being unable to react. This effect reduces the chance of undesirable termination by radical coupling. The segregation effect, therefore, increases the rate of polymerization.[58,61−64] In short, decreasing emulsion size which favors the segregation effect is expected to increase the rate of polymerization for the RAFT emulsion polymerization assuming the absence of diffusion. The same result was demonstrated by Monte Carlo simulation.[64] However, when diffusion is considered, a radical entry[64] or a radical loss (radical exit)[25,29,31,65,67,68] alters the polymerization kinetics. When the emulsion size is under 40 nm, radical entry into the emulsion becomes an important factor which may lead to rate retardation.[64] The leaving R group (this may include low-MW CTA leaving group) can exit from emulsions into the continuous phase, reducing the number of active radicals within the particle.[67]

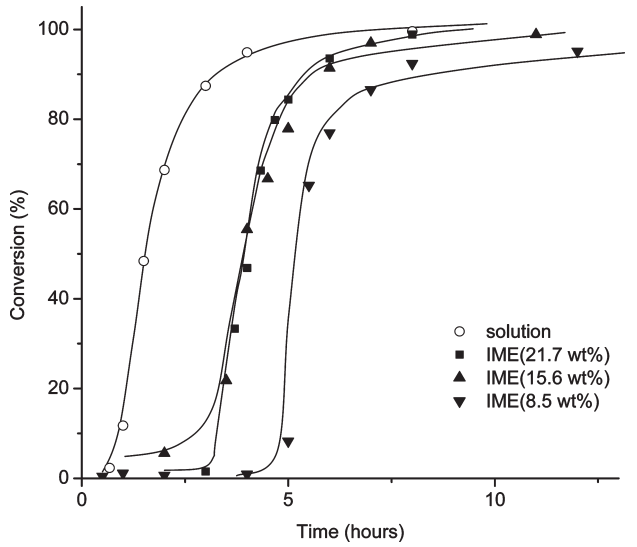

Figure 4. Time conversion plot of RAFT polymerization conducted in solution (○), IME (21.7 wt %) (■), IME (15.6 wt %) (▲), and IME (8.5 wt %) (▼).

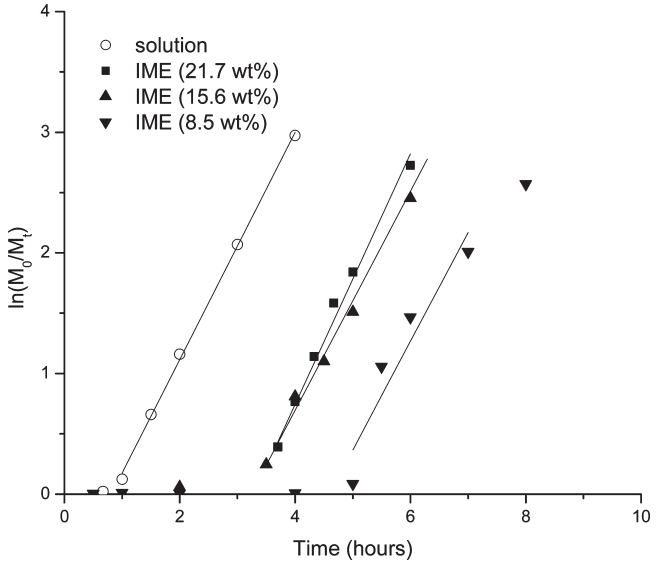

Figure 5. Kinetic plot of RAFT polymerization conducted in solution (○), IME (21.7 wt %) (■), IME (15.6 wt %) (▲), and IME (8.5 wt %) (▼).

Time versus conversion and pseudo-first-order kinetic plots are shown in Figures 4 and 5, respectively. For our RAFT-IMEPs, long induction periods are observed. One possible explanation for the induction period is radical loss (radical exit).[65,67] This has been observed previously in RAFT seeded emulsion polymerization,[25,29] and this effect was also thought to be responsible for rate retardation.[25,29,31,65,67,68] The CTA we used is slightly soluble in hexanes (the partition coefficient of CTA between oil phase and aqueous phase is 0.018 ($[CTA]_{oil}/[CTA]_{aq}$)). The induction period or rate retardation at very low conversion has been attributed to the oligomeric CTA reaching a critical length. Phase separation of oligomeric CTA has often been reported in O/W emulsion systems.[22,32,68] This is not observed under our IME conditions.

Once the polymerization starts as shown in Figure 5, the rate of polymerization is similar to or slightly faster than that of solution polymerization. There are no significant differences in the rates of polymerization with varying sizes of IMEs. The segregation and radical entry and loss have opposite effects on the rate of polymerization. However, a dispersed phase soluble initiator was used, and therefore rate retardation by a radical entry into the IME particle is assumed to be less likely. The radical loss effect may not be operative at moderate conversion because polymeric CTAs have poor solubility in the oil phase. For these reasons, the rates of polymerizations are similar to or slightly faster than aqueous solution polymerizations. Since this is the first report of RAFT-IMEP, interpretation of kinetic data can only be qualitative. Further research will be necessary to clarify additional issues related to the complicated RAFT mechanism.

Though the linearity of pseudo-first-order kinetic plots supports the livingness of the polymerization, this is not sufficient for the proof of controlled/living radical polymerization. To confirm the livingness of RAFT-IMEP, the molecular weight and PDI values at selected conversions were investigated. The results are shown in Figure 6. For RAFT solution polymerizations (Figure 6a), the experimental values of M_n agree well with the predicted theoretical values, with PDIs below 1.2. For the RAFT-IMEP with 21.7 wt % aqueous phase (Figure 6b) and 15.6 wt % aqueous phase (Figure 6c), the experimental values of M_n are higher than the theoretical values. However, both M_n's increased with conversion. PDIs remained below 1.2, even though they were higher at the initial stages of the polymerization. The differences between experimental M_n and theoretical values are attributed to the partitioning of CTA between the aqueous and continuous phases. This will be discussed further in a future paper.

GPC traces for the RAFT-IMEP with 15.6 wt % of aqueous phase are shown in Figure 7. These results indicate that these IMEPs are conducted in a controlled fashion. On the other hand, for the RAFT-IMEP with 8.6 wt % aqueous phase (Figure 6d), the experimental values of M_n are much larger than theoretical molecular weights. GPC traces were examined carefully in an attempt to identify the cause of this large PDI. GPC traces (RI detector) give a bimodal distribution shown in Figure 8a. The position of the lower M_n peak shifted to lower elution volume with increasing conversion while the position of higher M_n peak did not change. GPC traces from the UV detector (Figure 8b) overlap with the lower M_n peak of the RI curve. Since UV absorbance at 310 nm corresponds to the absorbance of the C=S bond in the CMP (RAFT CTA group), the lower M_n peak corresponds to a RAFT generated polymer. On the other hand, the higher M_n peak (shoulder) can be attributed to the uncontrolled polymerization or conventional polymerization of DMA in the absence of CTA, which likely occurs in the early stages of the polymerization.

Effect of the Number of CTAs in Each Particle on Polydispersity of Molecular Weight. When the polymerization is carried out in a confined space, the segregation effect, in theory, should reduce the chance of undesirable termination by radical coupling, improving PDIs.[24,69] In our case, the PDIs worsened with decreasing particle size of the IME. For the system with 8.5 wt % aqueous phase, uncontrolled polymer was generated. Two specific features about RAFT polymerization in microemulsion were proposed by Hermanson et al.[66] One is the generation of a local polymer concentration that is different from the average polymer concentration, caused by restricted diffusion of a polymer of certain chain length. The other feature is that the concentration of the unreacted CTA in the particle is not equal the concentration in the surrounding micelles. For a RAFT

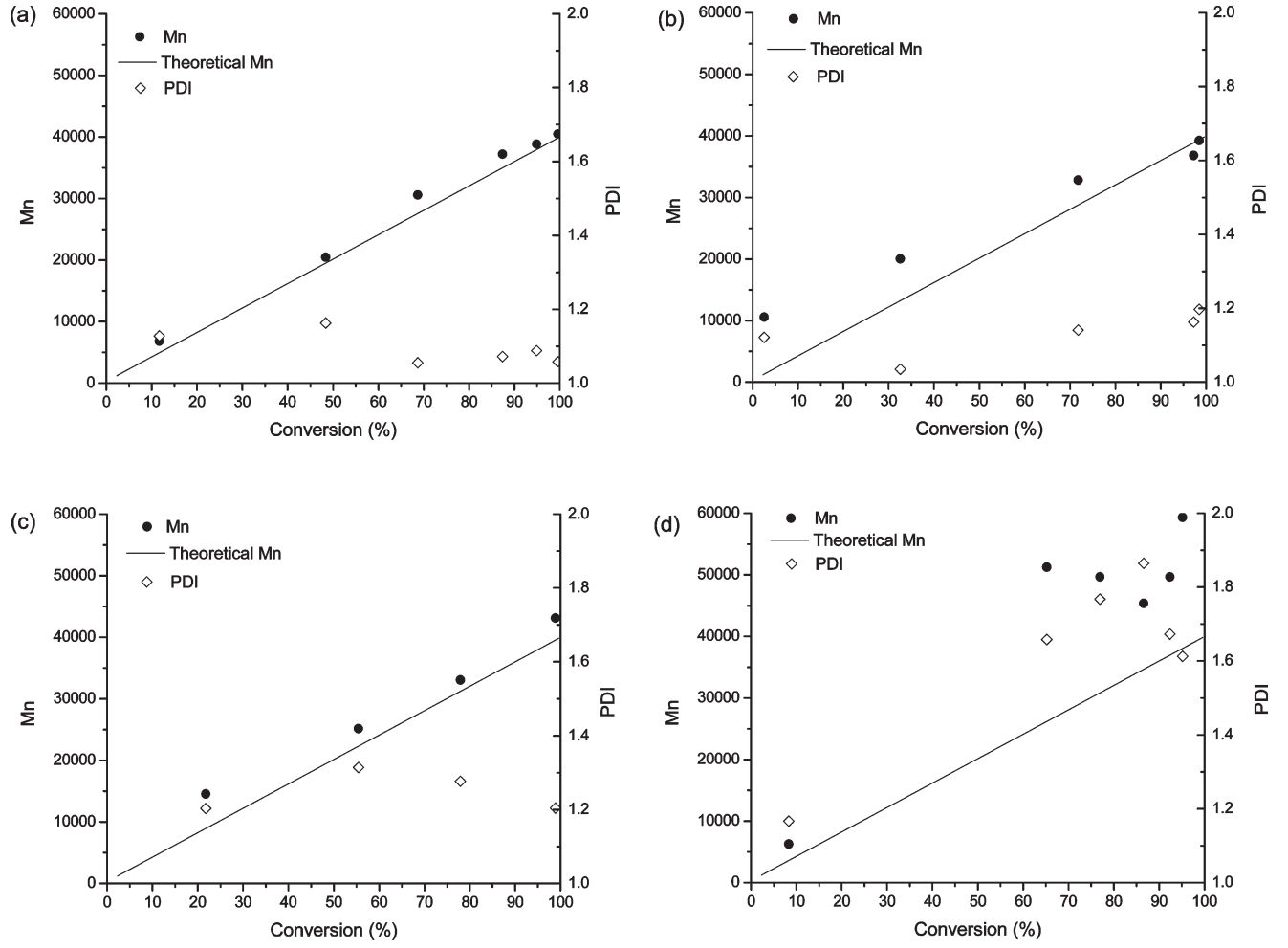

Figure 6. Number-average molecular weight (M_n) and polydispersity index (PDI) vs conversion for RAFT polymerizations (a) in solution, (b) IME (21.7 wt %), (c) IME (15.6 wt %), and (d) IME (8.5 wt %).

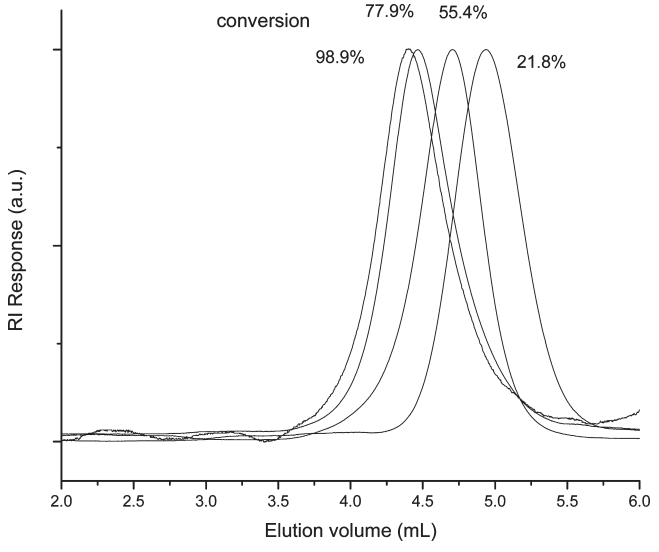

Figure 7. GPC chromatograms of RAFT-IMEP (15.6 wt % aqueous phase) by RI detection. Conversions are 21.8%, 55.4%, 77.9%, and 98.9%.

microemulsion system, the thermodynamic equilibrium involves the diffusion of monomer and CTA, even though their diffusion coefficients are not the same. Since these effects are enhanced by decreasing CTA concentration, higher concentrations of CTA (higher CTA in each IME) are needed to achieve the typical control that is generally observed in RAFT polymerization.[41,66] These two features appear to also be operative in RAFT-IMEP. The number of CTAs in each particle was calculated as shown in Table 3. The average number of CTAs per particle was found to be 2.7 for entry 5. Some IME particles may not contain any CTA at all. Therefore, the relative proportion of the monomer, CTA, and initiator might vary between particles at the early stages of the polymerization, and this could lead to the generation of uncontrolled polymer.

To confirm the effect of the number of CTAs in each particle, CTA concentration was doubled (entry 6) and quadrupled (entry 7). The average number of CTAs in each particle for entries 6 and 7 are 5.7 and 11.0, respectively. These lead to lower target molecular weights. As shown in Table 2, increasing CTA seems to affect the colloidal stability of the IME. The GPC traces are shown in Figure 9. The conversions of these entries are above 90% as shown in Table 2. The GPC chromatographs of entries 6 and 7 are unimodal with the absence of discernible shoulders. Both molecular weights are similar to predicted values and PDIs are narrower compared to entry 5. It is suggested that the number of CTAs in each particle has a significant effect on PDI of RAFT-IMEP. We are further investigating effects of concentration and CTA type on RAFT-IMEP.

Chain Extension and Block Copolymerization in One-Pot RAFT-IMEP. At the completion of the first RAFT-IMEP,

Table 3. Number of CTAs in Each Particle

entry	aqueous phase (wt %)	diameter (nm)	av no. of CTAs in each particle	av no. of initiators in each particle
3	21.7	19.5	11.9	2.4
4	15.6	18.3	9.7	1.9
5	8.5	11.9	2.7	0.5
6	8.5	11.3	5.7	1.1
7	8.5	11.7	11.0	2.2

Table 4. Chain Extension of PDMA with DMA by RAFT-IMEP

entry	aqueous phase (wt %)	DMA/CTA (mol/mol)	conv (%)	M_n(theory) (kg mol^{-1})	M_n(expt) (kg mol^{-1})	M_w/M_n	diameter (nm)
8-1	8.5	100	98.3	10.0	9.0	1.07	113.2
8-2	12.1	200	99.3	19.9	23.0	1.20	420.2

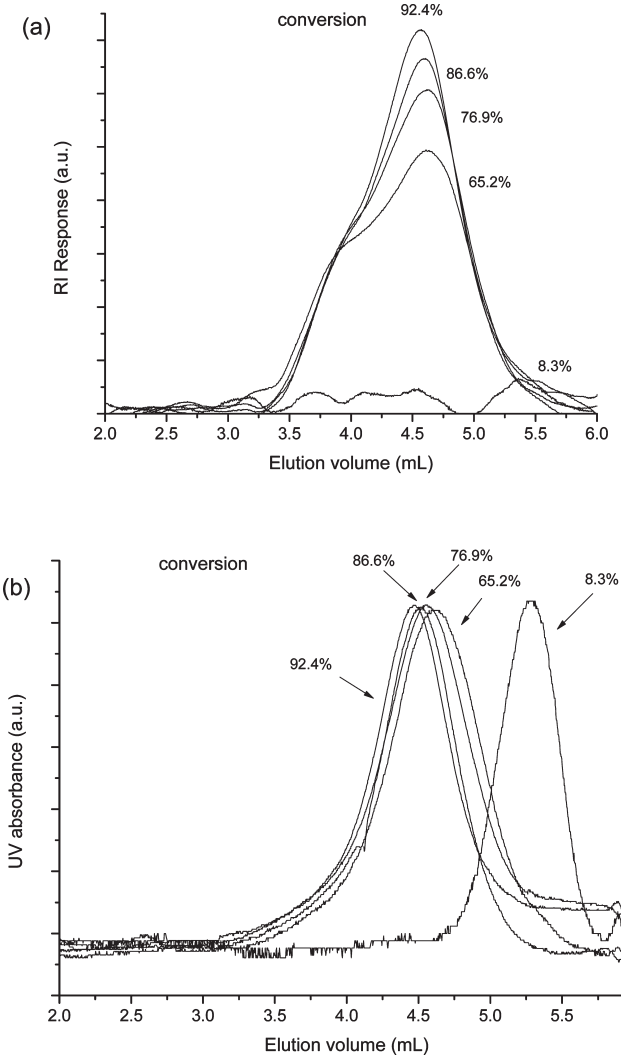

Figure 8. GPC chromatograms of RAFT-IMEP (8.5 wt %) by RI (a) and UV (b) detection. Conversions are 8.3%, 65.2%, 76.9%, 86.6%, and 92.4%.

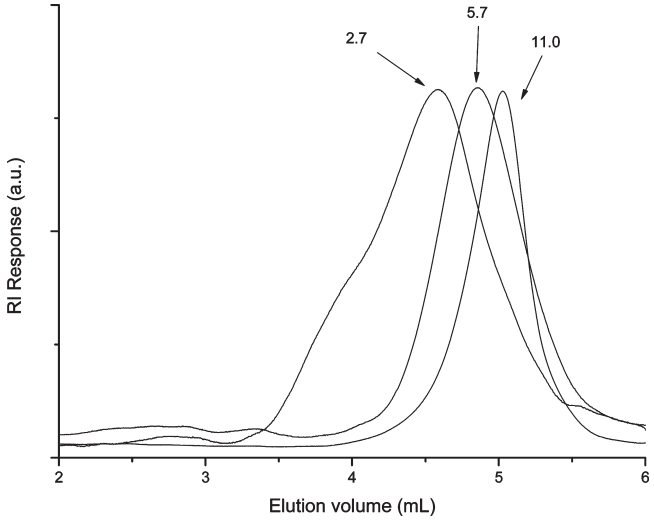

Figure 9. GPC chromatograms of RAFT-IMEP (8.5 wt %). The numbers of CTAs in each particle are 2.7, 5.7, and 11.0 at the beginning of polymerization, and the conversions of these GPC chromatograms are 96.5%, 92.2%, and 96.1%, respectively.

chain extension was conducted by directly adding a second batch of monomer into the IME mixture. The results are summarized in Table 4. Entry 8-1 shows the data for the seed inverse microemulsion while entry 8-2 contains the data after adding a second of batch of monomer to the seed IME. When a second batch of monomer was added, the diameter of IME increased (Table 4) from 113 to 420 nm. This increase in IME diameter could lead to the loss of particle stability as a result of monomer diffusion into the IME. Chain extension by this method is successful as indicated by the GPC chromatograms (before and after chain extension) shown in Figure 10. After chain extension, GPC traces shift to higher molecular weight, and a lower M_n peak (shoulder) is also observed. GPC traces monitored by UV (absorbance due to CTA moiety) match well with GPC traces determined by RI. Since the GPC traces by UV did not have a shoulder, the shoulder peak detected by RI can be attributed to the dead polymer of the first block. The molecular weight after chain extension agrees well with that theoretically predicted, and the PDI is below 1.3. The chain extension in RAFT-IMEP is well controlled. Moreover, no additional initiator was necessary in the chain extension experiment. We do not have an explanation for this observation at present. Since radicals are required to reactivate macroCTA, their source must be residual radicals or "stored" radicals, the latter suggested by Davis and co-workers.[70] Regardless of this mechanism not addressed further herein, chain extension may be applied for the synthesis of water-soluble block copolymers in properly formulated RAFT-IMEP systems.

In order to demonstrate the utility of this process, an ABA triblock copolymer was prepared by addition of *N,N*-diethylacrylamide (DEA) to the DMA macro-trithiocarbonate. A procedure similar to that utilized in chain extension was employed. The results are shown in Table 5. After 6 h polymerization, the conversion of the second monomer was 53.9%. The experimental chromatogram of the copolymer is shown in Figure 11. SEC was conducted with DMF as eluent, since polyDEA exhibits a lower critical solution

Table 5. Block Copolymerization of DMA and DEA by RAFT-IMEP

entry	aqueous phase (wt %)	DMA/CTA (mol/mol)	DMA/CTA (mol/mol)	conv (%)	M_n(theory) (kg mol^{-1})	M_n(expt) (kg mol^{-1})	M_w/M_n	diameter (nm)
9-1	8.5	100		95.4	9.0	9.4	1.05	102.2
9-2	10.6		106	53.9	16.9	13.2	1.07	179.7

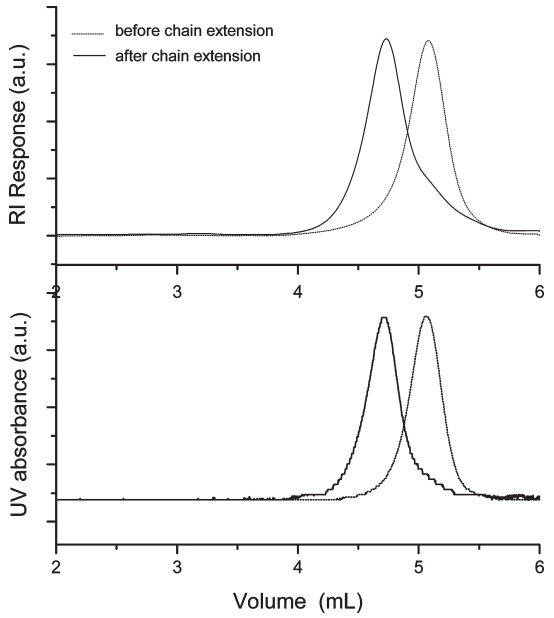

Figure 10. GPC chromatograms of RAFT-IMEP for the chain extension by RI and UV detection. The target DP of the first polymerization was 100 (98.3% conversion), and the final target DP after the chain extension was 200 (99.3% conversion).

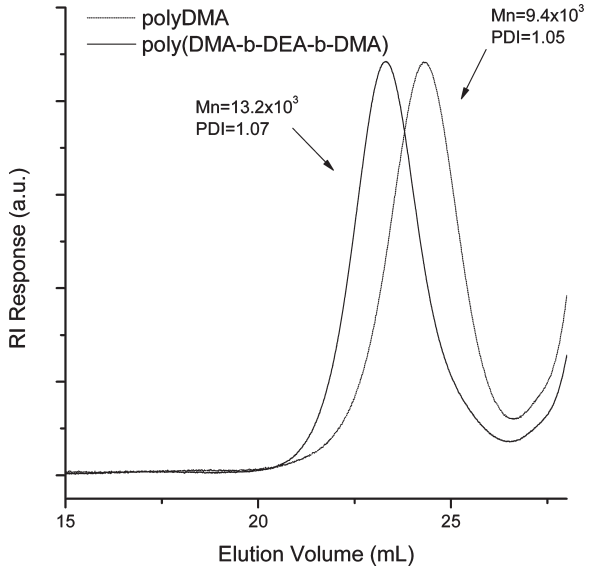

Figure 11. GPC chromatograms of poly(DMA-*b*-DEA-*b*-DMA) by RAFT-IMEP. The target structure of the first polymerization was polyDMA$_{100}$ (95.4% conversion), and the final target structure of the block copolymerization was poly(DMA$_{50}$-DEA$_{106}$-DMA$_{50}$) (53.9% conversion).

temperature at 30 °C. The chromatogram peak for the block copolymer shifts toward lower elution volume, and no shoulder due to the first block is observed. The peak at the elution volume of 27 mL is due to surfactants. This suggests successful block copolymerization in RAFT-IMEP. It should be noted that the experimental molecular weight is lower than that predicted based on complete retention of the macro-trithiocarbonate functionality.

Conclusions

RAFT inverse microemulsion polymerization (RAFT-IMEP) has been reported for the first time to our knowledge, resulting in well-controlled polymers retaining CTA functionality. The inverse microemulsion system reported herein was obtained by generating and optimizing pseudo-three-component phase diagrams utilizing the hydrophilic monomer *N,N*-dimethylacrylamide, water, hexanes, nonionic surfactants, and a cosurfactant. DMA and DMPA were utilized as cosurfactants to expand the inverse microemulsion region. The kinetic behavior and the living character of RAFT inverse microemulsion polymerization with systematic variation of the dispersed aqueous phase composition were compared to those of aqueous RAFT solution polymerization. The rate of polymerization of IMEP was similar to that in aqueous solution, although an induction period and a slight rate retardation at high conversion were observed. Decreasing the concentration of the dispersed aqueous phase led to an increase in colloidal stability and a decrease in microemulsion size. However, a point was reached where further decrease led to an increase in polydispersity, which may be due to uncontrolled radical-generated polymer formed at the early stage of the polymerization. Increasing the average number of CTAs in each particle was effective in achieving well-controlled RAFT polymerization. Chain extension and block copolymerization in RAFT-IMEP by sequential monomer addition were successfully accomplished. The monomers with similar characteristics have been utilized in these first examples. However, further studies are under way in our laboratories to assess the utility of preparing doubly hydrophilic and amphiphilic diblock copolymers with stimuli responsive properties utilizing this procedure.

References and Notes

(1) Hawker, C. J.; Bosman, A. W.; Harth, E. *Chem. Rev.* **2001**, *101*, 3661–3688.
(2) Matyjaszewski, K.; Xia, J. H. *Chem. Rev.* **2001**, *101*, 2921–2990.
(3) Perrier, S.; Takolpuckdee, P. *J. Polym. Sci., Part A: Polym. Chem.* **2005**, *43*, 5347–5393.
(4) Moad, G.; Rizzardo, E.; Thang, S. H. *Aust. J. Chem.* **2005**, *58*, 379–410.
(5) Lowe, A. B.; McCormick, C. L. *Prog. Polym. Sci.* **2007**, *32*, 283–351.
(6) McCormick, C. L.; Lowe, A. B. *Acc. Chem. Res.* **2004**, *37*, 312–325.
(7) Moad, G.; Chiefari, J.; Chong, Y. K.; Krstina, J.; Mayadunne, R. T. A.; Postma, A.; Rizzardo, E.; Thang, S. H. *Polym. Int.* **2000**, *49*, 993–1001.
(8) Rizzardo, E.; Chiefari, J.; Chong, B. Y. K.; Ercole, F.; Krstina, J.; Jeffery, J.; Le, T. P.; Mayadunne, R. T. A.; Meijs, G. F.; Moad, C. L.; Moad, G.; Thang, S. H. *Macromol. Symp.* **1999**, *143*, 291–307.
(9) Sumerlin, B. S.; Lowe, A. B.; Thomas, D. B.; McCormick, C. L. *Macromolecules* **2003**, *36*, 5982–5987.
(10) Vasilieva, Y. A.; Thomas, D. B.; Scales, C. W.; McCormick, C. L. *Macromolecules* **2004**, *37*, 2728–2737.
(11) Xu, X.; Smith, A. E.; Kirkland, S. E.; McCormick, C. L. *Macromolecules* **2008**, 8429–8435.
(12) Donovan, M. S.; Lowe, A. B.; Sanford, T. A.; McCormick, C. L. *J. Polym. Sci., Part A: Polym. Chem.* **2003**, *41*, 1262–1281.
(13) Li, Y.; Lokitz, B. S.; McCormick, C. L. *Macromolecules* **2006**, *39*, 81–89.
(14) Convertine, A. J.; Ayres, N.; Scales, C. W.; Lowe, A. B.; McCormick, C. L. *Biomacromolecules* **2004**, *5*, 1177–1180.

(15) Shah, D. O., Ed. *ACS Symp. Ser.* **1985**, *272*.
(16) Chou, Y. J.; El-Aasser, M. S.; Vanderhoff, J. W. *J. Dispersion Sci. Technol.* **1980**, *1*, 129–150.
(17) Ugelstad, J.; El-Aasser, M. S.; Vanderhoff, J. W. *J. Polym. Sci., Polym. Lett. Ed.* **1973**, *11*, 503–513.
(18) Le, T. P.; Moad, G.; Rizzardo, E. WO 9801478, **1998**.
(19) de Brouwer, H.; Tsavalas, J. G.; Schork, F. J.; Monteiro, M. J. *Macromolecules* **2000**, *33*, 9239–9246.
(20) Luo, Y. W.; Tsavalas, J.; Schork, F. J. *Macromolecules* **2001**, *34*, 5501–5507.
(21) Monteiro, M. J.; de Barbeyrac, J. *Macromolecules* **2001**, *34*, 4416–4423.
(22) Tsavalas, J. G.; Schork, F. J.; de Brouwer, H.; Monteiro, M. J. *Macromolecules* **2001**, *34*, 3938–3946.
(23) Monteiro, M. J.; de Brouwer, H. *Macromolecules* **2001**, *34*, 349–352.
(24) Butte, A.; Storti, G.; Morbidelli, M. *Macromolecules* **2001**, *34*, 5885–5896.
(25) Prescott, S. W.; Ballard, M. J.; Rizzardo, E.; Gilbert, R. G. *Macromolecules* **2002**, *35*, 5417–5425.
(26) Vosloo, J. J.; De Wet-Roos, D.; Tonge, M. P.; Sanderson, R. D. *Macromolecules* **2002**, *35*, 4894–4902.
(27) Ferguson, C. J.; Hughes, R. J.; Pham, B. T. T.; Hawkett, B. S.; Gilbert, R. G.; Serelis, A. K.; Such, C. H. *Macromolecules* **2002**, *35*, 9243–9245.
(28) Cunningham, M. F. *Prog. Polym. Sci.* **2002**, *27*, 1039–1067.
(29) Smulders, W.; Gilbert, R. G.; Monteiro, M. J. *Macromolecules* **2003**, *36*, 4309–4318.
(30) Cunningham, M. F. *Prog. Polym. Sci.* **2008**, *33*, 365–398.
(31) Prescott, S. W.; Ballard, M. J.; Rizzardo, E.; Gilbert, R. G. *Macromolecules* **2005**, *38*, 4901–4912.
(32) Huang, X. Y.; Sudol, E. D.; Dimonie, V. L.; Anderson, C. D.; El-Aasser, M. S. *Macromolecules* **2006**, *39*, 6944–6950.
(33) Smulders, W.; Monteiro, M. J. *Macromolecules* **2004**, *37*, 4474–4483.
(34) Freal-Saison, S.; Save, M.; Bui, C.; Charleux, B.; Magnet, S. *Macromolecules* **2006**, *39*, 8632–8638.
(35) Monteiro, M. J.; Sjoberg, M.; van der Vlist, J.; Gottgens, C. M. *J. Polym. Sci., Part A: Polym. Chem.* **2000**, *38*, 4206–4217.
(36) Luo, Y. W.; Gu, H. Y. *Polymer* **2007**, *48*, 3262–3272.
(37) Ferguson, C. J.; Hughes, R. J.; Nguyen, D.; Pham, B. T. T.; Gilbert, R. G.; Serelis, A. K.; Such, C. H.; Hawkett, B. S. *Macromolecules* **2005**, *38*, 2191–2204.
(38) Rieger, J.; Stoffelbach, F.; Bui, C.; Alaimo, D.; Jerome, C.; Charleux, B. *Macromolecules* **2008**, *41*, 4065–4068.
(39) Yang, L.; Luo, Y. W.; Li, B. G. *Polymer* **2006**, *47*, 751–762.
(40) Zhou, X. D.; Ni, P. H.; Yu, Z. Q. *Polymer* **2007**, *48*, 6262–6271.
(41) Liu, S. Y.; Hermanson, K. D.; Kaler, E. W. *Macromolecules* **2006**, *39*, 4345–4350.
(42) Leong, Y. S.; Candau, F. *J. Phys. Chem.* **1982**, *86*, 2641–2642.
(43) Leong, Y. S.; Candau, F. *J. Phys. Chem.* **1982**, *86*, 2269–2271.
(44) Candau, F.; Leong, Y. S.; Pouyet, G.; Candau, S. *J. Colloid Interface Sci.* **1984**, *101*, 167–183.
(45) Candau, F.; Leong, Y. S.; Fitch, R. M. *J. Polym. Sci., Polym. Chem. Ed.* **1985**, *23*, 193–214.
(46) Carver, M. T.; Hirsch, E.; Wittmann, J. C.; Fitch, R. M.; Candau, F. *J. Phys. Chem.* **1989**, *93*, 4867–4873.
(47) Barton, J.; Tino, J.; Hlouskova, Z.; Stillhammerova, M. *Polym. Int.* **1994**, *34*, 89–96.
(48) Juranicova, V.; Kawamoto, S.; Fujimoto, K.; Kawaguchi, H.; Barton, J. *Angew. Makromol. Chem.* **1998**, *258*, 27–31.
(49) Barton, J.; Capek, I. *Macromolecules* **2000**, *33*, 5353–5357.
(50) de Buruaga, A. S.; Capek, I.; De la Cal, J. C.; Asua, J. M. *J. Polym. Sci., Part A: Polym. Chem.* **1998**, *36*, 737–748.
(51) Qi, G.; Jones, C. W.; Schork, F. J. *Macromol. Rapid Commun.* **2007**, *28*, 1010–1016.
(52) Kaneda, I.; Sogabe, A.; Nakajima, H. *J. Colloid Interface Sci.* **2004**, *275*, 450–457.
(53) Kaneda, I.; Sogabe, A. *Colloids Surf., A* **2005**, *270*, 163–170.
(54) Kunieda, H.; Shinoda, K. *J. Dispersion Sci. Technol.* **1982**, *3*, 233–244.
(55) Shinoda, K. *Prog. Colloid Polym. Sci.* **1983**, *68*, 1–7.
(56) Beckman, E. J.; Smith, R. D. *J. Phys. Chem.* **1990**, *94*, 345–350.
(57) Chow, P. Y.; Gan, L. M. *Adv. Polym. Sci. 175*, 257−298.
(58) Zetterlund, P. B.; Kagawa, Y.; Okubo, M. *Chem. Rev.* **2008**, *108*, 3747–3794.
(59) Smith, W. V.; Ewart, R. H. *J. Chem. Phys.* **1948**, *16*, 592–599.
(60) Butte, A.; Stori, G.; Morbidelli, M. *33*, 3485−3487.
(61) Zetterlund, P. B.; Okubo, M. *Macromolecules* **2006**, *39*, 8859–8967.
(62) Zetterlund, P. B.; Okubo, M. *Macromol. Theory Simul.* **2007**, *16*, 221–226.
(63) Tobita, H. *Macromol. Theory Simul.* **2007**, *16*, 810–823.
(64) Tobita, H.; Yanase, F. *Macromol. Theory Simul.* **2007**, *16*, 476–488.
(65) Prescott, S. W.; Ballard, M. J.; Rizzardo, E.; Gilbert, R. G. *Macromol. Theory Simul.* **2006**, *15*, 70–86.
(66) Hermanson, K. D.; Liu, S. Y.; Kaler, E. W. *J. Polym. Sci., Part A: Polym. Chem.* **2006**, *44*, 6055–6070.
(67) Peklak, A. D.; Butté, A. *J. Polym. Sci., Part A: Polym. Chem.* **2006**, *44*, 6114–6135.
(68) Monteiro, M. J.; Hodgson, M.; Brouwer, H. D. *J. Polym. Sci., Part A: Polym. Chem.* **2000**, *38*, 3864.
(69) Yang, L.; Luo, Y.; Li, B. *J. Polym. Sci., Part A: Polym. Chem.* **2005**, *43*, 4972–4979.
(70) Barner-Kowollik, C.; Vana, P.; Quinn, J. F.; Davis, T. P. *J. Polym. Sci., Part A: Polym. Chem.* **2002**, *40*, 1058–1063.